Contribution from the Department of Hydrocarbon Chemistry, Faculty of Engineering, and the Department of Chemistry, Faculty of Science, Kyoto University, Kyoto 606, Japan

Electronic Structure of the Rh-Rh Bond in Dirhodium Tetracarboxylates from a Study of Electronic Spectra of Neutral Molecules and Their Cation Radicals

TAKAYOSHI SOWA,[1a] TAKASHI KAWAMURA,*[1a] TADAMASA SHIDA,[1b] and TEIJIRO YONEZAWA[1a]

Received June 22, 1982

Electronic absorption spectra of $Rh_2(O_2CR)_4L_2$ [R = Et, CF_3; L = H_2O, $HC(CH_2CH_2)_3N$, PPh_3, $P(c\text{-}C_6H_{11})_3$, $P(OPh)_3$, $P(OMe)_3$] and some of their cation radicals are examined. The intense absorption band in the near-ultraviolet region ($\bar{\nu}$ = (25-46) × 10^3 cm^{-1} and log ϵ = 4.0-4.7 for neutral complexes and $\bar{\nu}$ = (17-23) × 10^3 cm^{-1} and log ϵ = 4.0-4.3 for cationic complexes) is assigned to the intermetallic $\sigma \rightarrow \sigma^*$ transition. Ligand dependences of the transition energy and the intensity of this absorption band are interpreted with a bonding model constructed from a hypothesis that metal-ligand interactions are larger than intermetallic interactions. This valence model can also account qualitatively for the ligand dependences of the intermetallic bond distance and the stretching frequency of the intermetallic bond in dirhodium tetracarboxylates and the odd-electron distribution in their cation radicals. The odd electron of $Rh_2(O_2CMe)_4(H_2O)_2^{+\cdot}$ is suggested not to be accommodated in the σ_{RhRh} MO. The CO stretching frequency of $Rh_2(O_2CCF_3)_4(CO)_2$ is 7 cm^{-1} higher than that of the free carbon monoxide, showing that there is practically no π-type interactions between the metal and the carbonyl in this complex.

During the course of ESR studies of electronic structures of ion radicals of diamagnetic dinuclear complexes,[2] we have developed the hypothesis that metal-ligand (M-L) interactions are larger than intermetallic (M-M) interactions[2c] to explain ESR results and electronic structures obtained with molecular orbital (MO) calculations. Geometries of a wide variety of dirhodium tetracarboxylates,[3] $Rh_2(O_2CR)_4L_2$ (I), and related

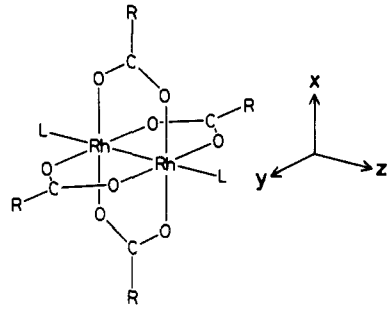

I

complexes[4a,b] have been studied to obtain insights into intermetallic and metal-ligand bonds. The knowledge of the geometry is the starting point of valence theory. We have examined the electronic structure of this class of complexes to determine whether these are consistent with our hypothesis.

The electronic spectrum of $Rh_2(O_2CMe)_4(H_2O)_2$ has been examined by Dubicki and Martin[4c] (Table I), who assigned observed absorption bands to $\pi^*_{RhRh} \rightarrow \sigma^*_{RhRh}$, $\pi^*_{RhRh} \rightarrow \sigma^*_{RhO}$, $\sigma_{RhRh} \rightarrow \sigma^*_{RhRh}$, and $\sigma_{RhO} \rightarrow$ Rydberg state transitions in the order of increasing energy. The assignment of the $\pi^*_{RhRh} \rightarrow \sigma^*_{RhRh}$ band has been confirmed by Martin and his co-workers[5] by examining single-crystal polarized absorption spectra. Norman and Kolari[6] have performed SCF-Xα-SW calculations of $Rh_2(O_2CH)_4(H_2O)_2$ and found that the intermetallic electronic configuration in the ground state is $\pi^4\sigma^2\delta^2\pi^{*4}\delta^{*2}$ with the HOMO of the δ^*_{RhRh} orbital. Their results support the assignments by Dubicki and Martin except that for the 45.9 × 10^3 cm^{-1} band, which Norman and Kolari attributed to the allowed $\sigma_{RhO} \rightarrow \sigma^*_{RhRh}$ transition.

Table I. Electronic Spectrum of $Rh_2(O_2CMe)_4(H_2O)_2$ in Water[a]

$\bar{\nu}_{max}/(10^3\ cm^{-1})$	ϵ^a	assignt[b]
17.1	241	$\pi^*_{RhRh} \rightarrow \sigma^*_{RhRh}$
22.7	106	$\pi^*_{RhRh} \rightarrow \sigma^*_{RhO}$
40 (sh)	~4000	$\sigma_{RhRh} \rightarrow \sigma^*_{RhRh}$
45.9	17000	$\sigma_{RhO} \rightarrow \sigma^*_{RhRh}$

[a] Wilson, C. R.; Taube, H. *Inorg. Chem.* 1975, *14*, 405. [b] Assignment based on SCF-Xα-SW calculations.[6a]

Scheme I

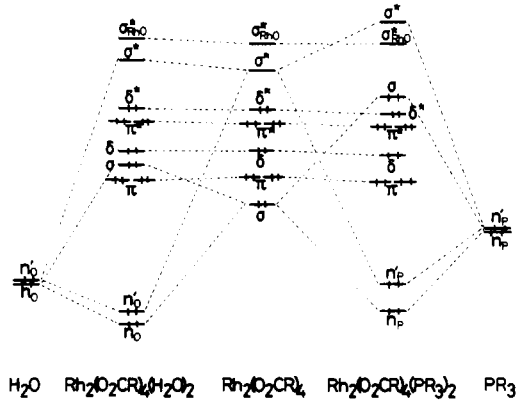

Our previous ESR study of $Rh_2(O_2CR)_4(PY_3)_2^{+\cdot}$[2a] shows that its odd-electron orbital is spread mainly over the Rh and P atoms and has σ_{RhRh} and σ^*_{RhP} characters (Scheme IB). This is supported by an SCF-Xα-SW calculation of $Rh_2(O_2CH)_4(PH_3)_2$ by Bursten and Cotton.[7] Nakatsuji and his

(1) (a) Department of Hydrocarbon Chemistry. (b) Department of Chemistry.
(2) (a) Kawamura, T.; Fukamachi, K.; Sowa, T.; Hayashida, S.; Yonezawa, T. *J. Am. Chem. Soc.* **1981**, *103*, 364. (b) Hayashida, S.; Kawamura, T.; Yonezawa, T. *Inorg. Chem.* **1982**, *21*, 2235. (c) Kawamura, T.; Enoki, S.; Hayashida, S.; Yonezawa, T., submitted for publication in *Bull. Chem. Soc. Jpn.*
(3) (a) Cotton, F. A.; DeBoer, B. G.; LaPrade, M. D.; Pipal, J. R.; Ucko, D. A. *Acta Crystallogr., Sect. A* **1971**, *A27*, 1664. (b) Christoph, G. G.; Koh, Y. B. *J. Am. Chem. Soc.* **1979**, *101*, 1422. (c) Koh, Y. B.; Christoph, G. G. *Inorg. Chem.* **1979**, *18*, 1122. (d) Cotton, F. A.; Felthouse, T. R. *Ibid.* **1980**, *19*, 2347; **1981**, *20*, 600, 2703. (e) Christoph, G. G.; Halpern, J.; Khare, G. P.; Koh, Y. B.; Romanowski, C. *Ibid.* **1981**, *20*, 3029. (f) Cotton, F. A.; Felthouse, T. R.; Klein, S. *Ibid.* **1981**, *20*, 3037.
(4) (a) Ziolkowsky, J. J.; Moszner, M.; Glowiak, T. *J. Chem. Soc., Chem. Commun.* **1977**, 760. (b) Cotton, F. A.; Felthouse, T. R. *Inorg. Chem.* **1981**, *20*, 584. (c) Dubicki, L.; Martin, R. L. *Ibid.* **1970**, *9*, 673.
(5) Martin, D. S., Jr.; Webb, T. R.; Robbins, G. A.; Fanwick, P. E. *Inorg. Chem.* **1979**, *18*, 475.
(6) (a) Norman, J. G., Jr.; Kolari, H. J. *J. Am. Chem. Soc.* **1978**, *100*, 791. (b) Norman, J. G., Jr.; Renzoni, G. E.; Case, D. A. *Ibid.* **1979**, *101*, 5256.
(7) Bursten, B. E.; Cotton, F. A. *Inorg. Chem.* **1981**, *20*, 3042.

0020-1669/83/1322-0056$01.50/0

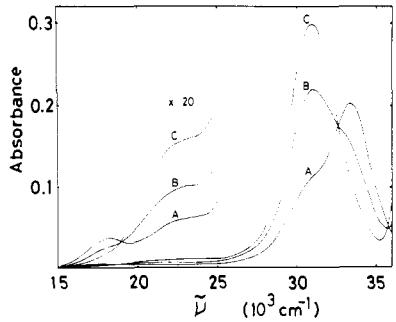

Figure 1. Absorption spectra of a 0.10 mmol L^{-1} solution of $Rh_2(O_2CEt)_4[P(OPh)_3]_2$ in CH_2Cl_2 containing (A) 0, (B) 0.2, and (C) 1.0 mmol L^{-1} of $P(OPh)_3$.

co-workers[8] have examined $Rh_2(O_2CH)_4L_2$ (L = H_2O, NH_3, PH_3) with ab initio Hartree–Fock calculations with a minimal STO-3G basis set and obtained a result that all the HOMO's of these three complexes are the σ_{RhRh} orbital with an appreciable σ^*_{RhL} character. Some discrepancies appear again between intermetallic bonding pictures given by SCF–Xα and Hartree–Fock methods. In response to the situation outlined above, we have examined electronic spectra of neutral molecules and cation radicals of phosphine and phosphite adducts of dirhodium tetracarboxylates and compared them with those of complexes with O- and N-centered axial ligands.

Results

Neutral Complexes. The electronic spectra of all the neutral dirhodium tetracarboxylates except those with aquo axial ligands are observed by dissolving them in dichloromethane. The aquo complexes are examined by using water as a solvent. Dirhodium complexes dissociate appreciably into a 1:1 adduct and a free ligand in dilute CH_2Cl_2 solutions:

$$Rh_2(O_2CR)_4L_2 \rightleftarrows Rh_2(O_2CR)_4L + L$$

For example, a 0.1 mmol L^{-1} solution of $Rh_2(O_2CEt)_4[P(OPh)_3]_2$ in CH_2Cl_2 shows two intense absorptions in the near-UV region (33.0×10^3 and 30.6×10^3 cm^{-1}) and a couple of weak bands in the visible region (21.5×10^3 and 17.5×10^3 cm^{-1}). Additions of excess phosphite to this solution result in an increase of intensities of the bands at 30.6×10^3 and 21.5×10^3 cm^{-1} at the sacrifice of those at 33.0×10^3 and 17.5×10^3 cm^{-1} (Figure 1). This is consistent with an equilibrium of adduct formation of $Rh_2(O_2CPr)_4$ with a base[9] and shows that absorptions with maxima at 33.0×10^3 and 17.5×10^3 cm^{-1} are due to the 1:1 adduct and those at 30.6×10^3 and 21.5×10^3 cm^{-1} arise from the 1:2 adduct.

Electronic spectra of all the complexes with N- or P-centered ligands show behavior similar to that of $Rh_2(O_2CEt)_4[P(OPh)_3]_2$ upon additions of excess of axial ligands, but the spectrum of $Rh_2(O_2CCF_3)_4(PPh_3)_2$ changes slowly ($t_{1/2} \simeq 4$ min) probably due to a decomposition of this complex. Spectral data are summarized in Table II.

Cation Radicals. Cation radicals of $Rh_2(O_2CEt)_4(PPh_3)_2$ and $Rh_2(O_2CEt)_4(P(Cy)_3)_2$ (Cy = cyclohexyl) were obtained by electrochemical oxidation of their parent neutral complexes in CH_2Cl_2 solution containing n-Bu_4NClO_4 as a supporting electrolyte. The former complex is known to be oxidized into a cation radical by electrolysis at 0.75 V vs. SCE.[2a] Cyclic voltammetry of the latter complex shows a quasi-reversible one-electron oxidation peak at 0.24 V vs. SCE. Coulometry and ESR of the electrolyte solution of the latter complex after a controlled-potential electrolysis at 0.3 V vs. SCE in CH_2Cl_2 confirm the electrochemical one-electron oxidation of the complex. The electronic spectrum for $Rh_2(O_2CEt)_4(P(Cy)_3)_2^{+\cdot}$ generated by electrolysis is shown in Figure 2.

Table II. Absorption Spectra of $Rh_2(O_2CR)_4L_2^{0,+}$

R	L	charge[a]	$\bar{\nu}_{max}/(10^3$ cm$^{-1})$ [no.,[b] log ϵ]
Et	PPh_3	0[c]	27.3 [1, 4.59], 20.0 (sh) [2, 3.15]
Et	$P(Cy)_3$[d]	0[c]	28.3 [1, 4.54], 20.4 (sh) [2, 2.85]
Et	$P(OMe)_3$	0[c]	30.7 [1, 4.41], 21.7 (sh) [2, 2.85]
Et	$P(OPh)_3$	0[c]	31.0 [1, 4.48], 21.5 (sh) [2, 2.78]
Et	quin[e]	0[c]	34.8 [1, 4.40], 31.3 (sh) [2, 3.46], 19.2 [3, 2.48]
Et	H_2O	0[f]	45.9 [1, 4.08], 38.5 (sh) [2, 3.63], 22.5 [3, 2.07], 17.2 [4, 2.30]
CF_3	PPh_3	0[c]	25.1 [1, 4.63], (21.5 (sh) [2, 3.7][g])
CF_3	$P(OPh)_3$	0[c]	28.6 [1, 4.54], 21.3 (sh) [2, 3.15]
CF_3	quin[e]	0[c]	31.8 [1, 4.49], 20.0 [2, 2.5]
CF_3	H_2O	0[f]	44.6 [1, 4.08], 38.5 (sh) [2, 3.56], 22.2 [3, 1.97], 17.3 [4, 2.21]
Et	PPh_3	+[c,h]	18.6 [1, 4.40]
Et	$P(Cy)_3$[d]	+[c,h]	23.0 [1, 4.61], 19.2 [2, 4.28]
Et	PPh_3	+[i]	19.2 [1, 4.0], 18.5 (sh) [2, 3.9]
Et	$P(Cy)_3$[d]	+[i]	23.0 [1, 4.3], 19.4 [2, 3.8]
Et	$P(OPh)_3$	+[i]	22.2 [1, 4.3], 15.6 (br)[k] [2, 3.6]
Et	$P(OMe)_3$	+[i]	21.5 [1, 4.0], 17.2 (br)[k] [2, 3.3]
Me	H_2O	+[f,j]	45.8 [1, 4.11], 40.0 [2, 3.95], 30.3 [3, 3.08], 19.3 [4, 2.34], 13.1 [5, 2.33]
CF_3	PPh_3	+[i]	17.3 [1, 4.0], 14.9 (sh) [2, 3.6]
CF_3	$P(OPh)_3$	+[i]	20.5 [1, 4.0], 14.3 (br)[k] [2, 3.5]

[a] Legend: 0, neutral complex; +, cation radical. [b] Numbering of band. [c] At room temperature in CH_2Cl_2. [d] Cy = cyclohexyl. [e] Quin = quinuclidine. [f] At room temperature in H_2O. [g] Observed at 77 K in glassy frozen Freon mixture. This shoulder was not resolved at room temperature. [h] Generated by electrolysis. [i] At 77 K in frozen Freon mixture; generated by radiolysis. The reported values of log ϵ_{max} should be regarded as its lower limit (see text). [j] Moszner, M.; Ziolkowski, J. J. *Bull. Acad. Pol. Sci., Ser. Sci. Chim.* 1976, *24*, 433. [k] Broad band.

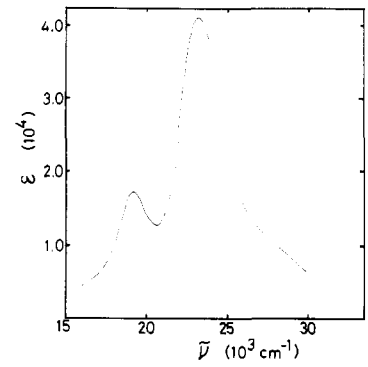

Figure 2. Absorption spectrum of electrochemically generated $Rh_2(O_2CEt)_4(P(Cy)_3)_2^{+\cdot}$ (0.08 mmol L^{-1}) in CH_2Cl_2 at room temperature. The electrolyte solution contains 1.0 mmol L^{-1} of $P(Cy)_3$ to suppress the equilibrium toward the 1:1 complex and 0.1 mol L^{-1} of n-Bu_4NClO_4 as a supporting electrolyte.

Cation radicals of complexes with P-centered axial ligands are generated also by γ-ray irradiations. The glassy frozen Freon mixture ($CFCl_3$:CF_2BrCF_2Br = 1:1 v/v) has been shown to be an appropriate matrix for trapping cation radicals of solutes formed upon radiolysis.[2a,10] It has no absorption band in the visible region[10] allowing optical measurements of solute cations. The change of the absorption spectrum in the visible region induced by γ irradiation of a frozen Freon mixture containing a complex can thus be attributed to the spectrum of the solute cation. Figure 3 shows the spectrum

(8) Nakatsuji, H.; Ushio, J.; Kanda, K.; Onishi, Y.; Kawamura, T.; Yonezawa, T. *Chem. Phys. Lett.* **1981**, *79*, 299.
(9) Drago, R. S.; Tanner, S. P.; Richman, R. M.; Long, J. R. *J. Am. Chem. Soc.* **1979**, *101*, 2897.
(10) (a) Shida, T.; Iwata, S. *J. Am. Chem. Soc.* **1973**, *95*, 3473. (b) Shida, T.; Kato, T.; Nosaka, Y. *J. Phys. Chem.* **1977**, *81*, 1095. (c) Kato, T.; Shida, T. *J. Am. Chem. Soc.* **1979**, *101*, 6869.

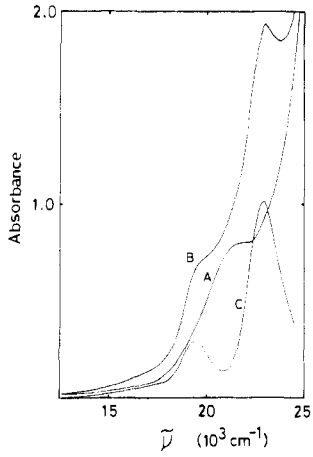

Figure 3. Absorption spectra of a frozen (77 K) Freon mixture solution of $Rh_2(O_2CEt)_4(P(Cy)_3)_2$ observed (A) before and (B) after radiolysis. Spectrum C is due to $Rh_2(O_2CEt)_4(P(Cy)_3)_2^{+\cdot}$ at 77 K obtained as (B) − (A).

of $Rh_2(O_2CEt)_4(P(Cy)_3)_2^{+\cdot}$ generated by radiolysis, which coincides with that of the electrochemically generated cation radical shown in Figure 2.

For the estimation of ϵ values of a radiochemically generated cation, the concentration of cationic species, C (mol L^{-1}), was determined by using the equation[10]

$$C = 10Gt\rho(\mathrm{DR})/N$$

where G is the ionization G value of the Freon mixture (2.09 molecules/100 eV[10]), N is Avogadro's number, DR is the dose rate in the unit of eV min^{-1} g^{-1}, ρ is the density of the Freon mixture (2.28 g mL^{-1} at 77 K[10]), and t is the time of irradiation in minutes. This equation assumes that all the positive holes generated in the frozen Freon mixture upon radiolysis are transferred to solute molecules. The value of C obtained with this equation is, therefore, an overestimate. Thus we can determine only the lower limit of ϵ by this method.

Cation radicals with axial ligands of a phosphine or a phosphite show two relatively intense absorptions in the visible region. Spectral data of cationic complexes are also listed in Table II.

Discussion

$\sigma \rightarrow \sigma^*$ Transition of the Neutral Complex. The lowest energy transitions in the electronic spectrum of $Rh_2(O_2CH)_4(PH_3)_2$ have been predicted by Bursten and Cotton[7] on the basis of SCF–Xα–SW calculations to be the $\sigma_{RhRh} \rightarrow \sigma^*_{RhO}$ (allowed $a_g \rightarrow b_u$ in C_{2h}; forbidden $a_{1g} \rightarrow b_{2u}$ in D_{4h}) and the $\sigma_{RhRh} \rightarrow \sigma^*_{RhRh}$ (allowed $a_g \rightarrow b_u$ in C_{2h}; allowed $a_{1g} \rightarrow a_{2u}$ in D_{4h}) transitions at 14.8×10^3 and 16.4×10^3 cm^{-1}, respectively, which are isolated from other allowed (in C_{2h}) transitions by about 10×10^3 cm^{-1}. In accordance with the prediction, two absorption bands are found below 43×10^3 cm^{-1} in spectra of dirhodium tetracarboxylates with axial ligands of P-centered bases. One (band 1 in Table II) is a very intense band with log ϵ_{max} greater than 4, and the other (band 2 in Table II) is a rather weak band observed as a shoulder on band 1.

On the basis of these SCF–Xα–SW calculations and the fact that intermetallic $\sigma \rightarrow \sigma^*$ transitions in dinuclear transition-metal carbonyls have been known to have log ϵ_{max} values greater than 4,[11] we assign band 1 of the neutral dirhodium complexes with P-centered axial ligands to the intermetallic

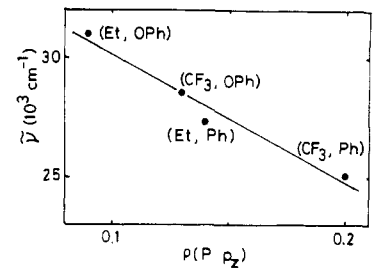

Figure 4. Relation between the $\sigma_{RhRh} \rightarrow \sigma^*_{RhRh}$ band (band 1) maxima of $Rh_2(O_2CR)_4(PY_3)_2$ and odd-electron density on the phosphorus $3p_z$ AO in $Rh_2(O_2CR)_4(PY_3)_2^{+\cdot}$. The notations (R, Y) designate the complexes.

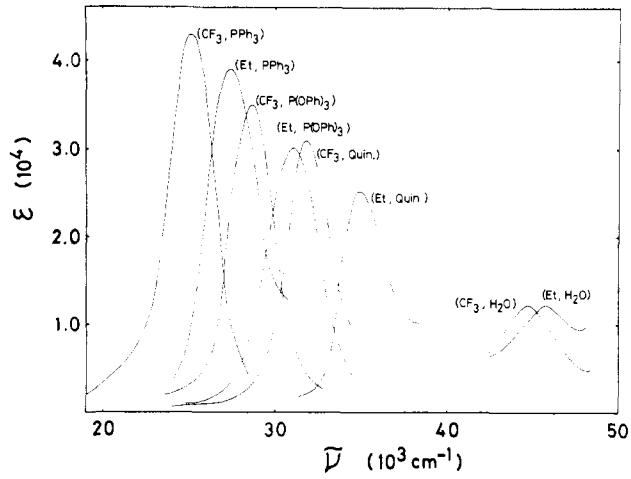

Figure 5. $\sigma_{RhRh} \rightarrow \sigma^*_{RhRh}$ absorptions in $Rh_2(O_2CR)_4L_2$. The notations (R, L) designate the complexes.

$\sigma \rightarrow \sigma^*$ transition. Support for this assignment comes from a correlation between the absorption maximum of band 1 of a $Rh_2(O_2CR)_4(PY_3)_2$ complex and the experimental odd-electron density[2a] on the phosphorus $3p_z$ AO, $\rho(P\ p_z)$, in the corresponding cation radical, $Rh_2(O_2CR)_4(PY_3)_2^{+\cdot}$ (Figure 4). Our previous ESR study of $Rh_2(O_2CR)_4(PY_3)_2^{+\cdot}$[2a] shows that the σ_{RhRh} MO has large components of the lone-pair orbital of the axial ligands in an antibonding phase with respect to the Rh–P σ interaction and that the extent of the mixing depends on the σ donor strength of the ligands. Because of the antibonding phase, an increase of the lone-pair orbital component (namely, the increase of $\rho(P\ p_z)$) is expected to be accompanied by an upward shift of the σ_{RhRh} orbital energy and therefore with a decrease of the $\sigma_{RhRh} \rightarrow \sigma^*_{RhRh}$ transition energy (see Scheme I). This expectation is satisfied as shown in Figure 4, supporting the present assignment.

The intermetallic $\sigma \rightarrow \sigma^*$ transition of $Rh_2(O_2CMe)_4(H_2O)_2$ was assigned to the weak absorption at 40×10^3 cm^{-1} observed as a shoulder on an intense band at 45.9×10^3 cm^{-1}, which was attributed to the allowed $\sigma_{RhO} \rightarrow \sigma^*_{RhRh}$ ($a_g \rightarrow b_{1u}$ in C_{2h}, $a_{1g} \rightarrow a_{2u}$ in D_{4h}) transition (Table I). However, we prefer to assign the 45.9×10^3 cm^{-1} band to the $\sigma_{RhRh} \rightarrow \sigma^*_{RhRh}$ transition because of the following two reasons. First, the log ϵ_{max} value of 4.23 of this band is more consistent with those of the $\sigma_{RhRh} \rightarrow \sigma^*_{RhRh}$ bands of the complexes with P-centered ligands. Second, upon substitution of the bridging ligand from acetate to trifluoroacetate, this band shows an appreciable red shift (45.9×10^3 cm^{-1} in the acetate to 44.6×10^3 cm^{-1} in the trifluoroacetate; Tables I and II), which parallels the red shift of the $\sigma_{RhRh} \rightarrow \sigma^*_{RhRh}$ transition of the $Rh_2(O_2CR)_4(PY_3)_2$ complexes observed upon the substitution of the carboxylate ligands. The σ_{RhO} orbital is mainly the a_{1g} (in D_{4h}) combination of the lone-pair orbitals on the carboxylate oxygen atoms expanding toward rhodium atoms with minor in-phase

(11) (a) Levenson, R. A.; Gray, H. B. *J. Am. Chem. Soc.* **1975**, *97*, 6042. (b) Abrahamson, H. B.; Frazier, C. C.; Ginley, D. S.; Gray, H. B.; Lilienthal, J.; Tyler, D. R.; Wrighton, M. S. *Inorg. Chem.* **1977**, *16*, 1554.

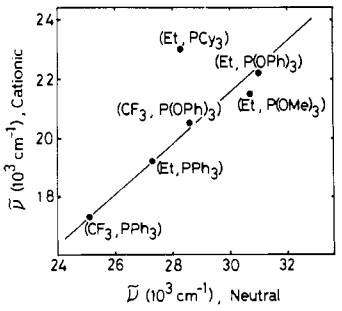

Figure 6. Relation between $\sigma_{RhRh} \rightarrow \sigma^*_{RhRh}$ transition energies of $Rh_2(O_2CR)_4(PY_3)_2^{+\cdot}$ and $Rh_2(O_2CR)_4(PY_3)_2$.

components of rhodium atomic orbitals. When the bridging carboxylate is substituted from acetate to trifluoroacetate, the energy level of the σ_{RhO} orbital is expected to shift downward, thus resulting in a blue shift of the $\sigma_{RhO} \rightarrow \sigma^*_{RhRh}$ transition, contrary to the experimental results.

Thus we assign band 1 of all the neutral complexes in Table II to the $\sigma_{RhRh} \rightarrow \sigma^*_{RhRh}$ transition. The log ϵ_{max} values of this band are greater than 4. Upon an increase of σ donor strength of axial ligands, this band shows a red shift. When bridging ligands are substituted from propionate to trifluoroacetate, this band shows a red shift of (1–3) $\times 10^3$ cm^{-1}. Figure 5 summarizes the $\sigma_{RhRh} \rightarrow \sigma^*_{RhRh}$ band of each of the neutral complexes. An increase of the transition energy is accompanied by a decrease of the band intensity.

$\sigma_{RhRh} \rightarrow \sigma^*_{RhRh}$ Transition of the Cation Radical. The $\sigma_{RhRh} \rightarrow \sigma^*_{RhRh}$ ($^2A_g \rightarrow {}^2B_u$ in C_{2h}) transition energy and its oscillator strength of $Rh_2(O_2CH)_4(PH_3)_2^{+\cdot}$ were predicted to be 29.8 $\times 10^3$ cm^{-1} and 0.599, respectively, by the ΔSCF method with ab initio Hartree–Fock MO calculations with a double-ζ basis set.[12] On the basis of this prediction, we assign band 1 of $Rh_2(O_2CR)_4(PY_3)_2^{+\cdot}$ to the $\sigma_{RhRh} \rightarrow \sigma^*_{RhRh}$ transition. This assignment is supported by the linear relation between their absorption maxima of band 1 and the $\sigma_{RhRh} \rightarrow \sigma^*_{RhRh}$ transition energies of their corresponding parent neutral complexes (Figure 6). The $\sigma_{RhRh} \rightarrow \sigma^*_{RhRh}$ transition energy of $Rh_2(O_2CR)_4(PY_3)_2^{+\cdot}$ is about 8 $\times 10^3$ cm^{-1} smaller than that of the neutral complex. Since an electron is ionized from the orbital with σ_{RhRh} and σ^*_{RhP} characteristics,[2a] the Rh–Rh bond length of the cation should be longer than that of the neutral complex and the Rh–P bond length of the cation is expected to be shorter than that of the neutral complex. Both of these geometrical changes upon the ionization should result in the red shift of the $\sigma_{RhRh} \rightarrow \sigma^*_{RhRh}$ transition band.

If we assume that $Rh_2(O_2CMe)_4(H_2O)_2^{+\cdot}$ has its odd electron in the σ_{RhRh} MO, the absorption at 45.8 $\times 10^3$ cm^{-1} should be assigned to the $\sigma_{RhRh} \rightarrow \sigma^*_{RhRh}$ transition. However, since this band does not show the red shift mentioned above from that of the neutral complex (Tables I and II), we suggest that the odd electron of $Rh_2(O_2CMe)_4(H_2O)_2^{+\cdot}$ is not accommodated in the σ_{RhRh} MO.

Model of Bonding. We have constructed a model to describe the intermetallic bonding in the present type of complexes. The model is based on the hypothesis that M–L interactions are greater than M–M interactions. The experimental results are compared with the results predicted by this bonding model. Larger interactions are considered first; weaker ones are taken into account thereafter. The model is of an electronic structure for a mononuclear unit with a square-pyramidal C_{4v} geometry, and then two mononuclear units are combined through M–M interactions into a dinuclear complex with a D_{4h} geometry.

The construction of the bonding scheme starts from a d^7 Rh(II) ion surrounded by four oxygen atoms (of bridging carboxylates) in a square-planar D_{4h} geometry (**1** in Figure 7). The MO with dominant $d_{x^2-y^2}$ character has the highest orbital energy among the five d MO's because of strong antibonding characteristics between the $d_{x^2-y^2}$ atomic orbital (AO) and oxygen lone-pair orbitals expanding toward the metal atom. (We give a name of "$d_{x^2-y^2}$ MO" to this orbital, and so on.) The orbital energy ordering of the other four d MO's are sketched as $d_{xz} = d_{yz} < d_{z^2} < d_{xy}$ by assuming carboxylate ligands are σ donative as well as π donative, but this ordering can also be $d_{xz} = d_{yz} < d_{xy} < d_{z^2}$. Since trifluoroacetate is a poor σ donor in comparison to the propionate ligand, the energy of the d_{z^2} MO would be less destablized in complex **1** with trifluoroacetate ligands than that with propionate ligands.

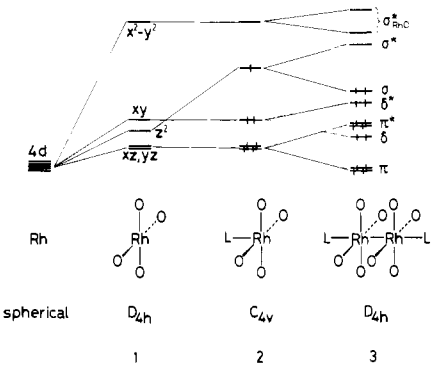

Figure 7. Formation of intermetallic orbitals of $Rh_2(O_2CR)_4L_2$ from d orbitals of mononuclear units.

When the axial ligand L is added to **1** to form the square-pyramidal complex **2**, the energy of the d_{z^2} MO shifts upward due to the anti-phase mixing of the σ lone-pair orbital on L, n_L.

When two mononuclear units, **2**, are combined together to form a D_{4h} dinuclear complex, **3**, intermetallic σ and σ^*, doubly degenerate π and π^*, and δ and δ^* MO's are formed through d–d interactions from pairs of d_{z^2}, d_{xz} and d_{yz}, and d_{xy} MO's, respectively. In the dinuclear complex, **3**, 2 × 7 = 14 "d electrons" occupy seven lower intermetallic MO's, resulting in a net single σ intermetallic bond. Depending on the relative energy level of the d_{z^2} MO in **2** and the orbital energy splitting between σ and σ^* MO's in **3**, the σ^* MO may be located below or above the σ^*_{RhO} MO,[6,7] and the σ MO may be located below or above other doubly occupied intermetallic MO (MO's)[6,7,13] in the energy diagram for **3**.

The d_{z^2} MO of **2**, ψ_{z^2}, can be represented as the d_{z^2} AO with antiphase contaminants of n_L and n_O:

$$\psi_{z^2} = C_{Rh}d_{z^2} - C_L n_L - C_O n_O \qquad (1)$$

where n_O designates the normalized a_1 (in C_{4v}) combination of four oxygen lone pairs expanding toward the metal atom. An increase of σ donor strength of L (i.e., $H_2O <$ Quin $< P(OR)_3 < PR_3$) induces an upward shift of the energy of the d_{z^2} MO, a decrease of C_{Rh}, and an increase of C_L. When the bridging ligand is substituted from propionate to less σ donative trifluoroacetate, C_L increases at the sacrifice of C_{Rh}, because this substitution decreases the orbital energy separation between n_L and the d_{z^2} MO.

The intermetallic σ and σ^* MO's are in-phase and antiphase combinations of $\psi_{z^2(1)}$ and $\psi_{z^2(2)}$, respectively, where the additional subscripts of 1 and 2 represent the right-side and the left-side moieties of the dinuclear complex, respectively:

(12) Nakatsuji, H.; Onishi, Y.; Ushio, J.; Yonezawa, T., to be submitted for publication.

(13) An orbital energy ordering of $\delta < \pi < \pi^* < \sigma < \delta^* < \sigma^*$ for $Rh_2(O_2CH)_4(H_2O)_2$ has been obtained by an ab initio Hartree–Fock calculation with a double-ζ STO-3G basis set.[12]

$$\sigma = (1/2)^{1/2}(\psi_{z^2(1)} + \psi_{z^2(2)})$$

$$= (1/2)^{1/2}[C_{Rh}(d_{z^2(1)} + d_{z^2(2)}) - C_L(n_{L(1)} + n_{L(2)}) - C_O(n_{O(1)} + n_{O(2)})] \quad (2)$$

$$\sigma^* = (1/2)^{1/2}(\psi_{z^2(1)} - \psi_{z^2(2)})$$

$$= (1/2)^{1/2}[C_{Rh}(d_{z^2(1)} - d_{z^2(2)}) - C_L(n_{L(1)} - n_{L(2)}) - C_O(n_{O(1)} - n_{O(2)})] \quad (3)$$

With these MO's, the $\sigma \rightarrow \sigma^*$ transition energy, ΔE, and the oscillator strength for this transition, f, are given as

$$\Delta E = \langle \sigma^*|\mathcal{H}|\sigma^*\rangle - \langle \sigma|\mathcal{H}|\sigma\rangle \simeq -2C_{Rh}^2\langle d_{z^2(1)}|\mathcal{H}|d_{z^2(2)}\rangle \quad (4)$$

$$f = k|\langle \sigma|\mathcal{R}|\sigma^*\rangle|^2 \simeq (k/2)[C_{Rh}^2R_{RhRh} + C_L^2R_{LL} + C_O^2R_{OO}] \quad (5)$$

where k is a constant, $\mathcal{H}$ is the total Hamiltonian, $\langle d_{z^2(1)}|\mathcal{H}|d_{z^2(2)}\rangle$ is the resonance integral between the neighboring rhodium d_{z^2} AO's in a simple MO theory and is negative, and R_{RhRh}, R_{LL}, and R_{OO} are interatomic distances between pairs of the Rh atoms, between the central atoms of the axial ligands, and between the oxygen atoms of the carboxylate, respectively. Relative magnitudes of interatomic distances are $R_{OO} \lesssim R_{RhRh} << R_{LL}$.[3]

Some qualitative expectations for ligand dependences of physicochemical properties of $Rh_2(O_2CR)_4L_2$ can be derived from the present bonding scheme. These expectations arise simply from ligand dependences of magnitudes of C_{Rh} and C_L in ψ_{z^2} (eq 1) of the mononuclear unit, **2**.

When the σ donor strength of the axial ligand is increased or when the donor strength of the bridging carboxylate is decreased, the following predictions can be made: (i) The $\sigma \rightarrow \sigma^*$ transition energy is predicted to decrease because of the expected decrease of C_{Rh} (eq 4). (ii) The intensity of the $\sigma \rightarrow \sigma^*$ transition band is expected to increase due to the expected increase of C_L and decrease of C_{Rh} (eq 5). We would like to point our that Scheme I cannot give this type of simple prediction on the intensity of this band unless some type of calculations are carried out. (iii) The odd-electron density on the Rh d_{z^2} AO, C_{Rh}^2, of $Rh_2(O_2CR)_4(PY_3)_2^{+\cdot}$, in which the odd electron occupies the σ_{RhRh} MO,[2a] is expected to decrease, and that on the axial ligand lone-pair orbital, C_L^2, is predicted to increase. (iv) The intermetallic bond distance is expected to increase. This prediction is based on the assumption that the distance is inversely correlated with the intermetallic bond order, which is equal to C_{Rh}^2 in the present simplified bonding scheme.

Predictions i and ii are consistent indeed with the experimental results visualized in Figure 5. Prediction iii is consistent with the ESR results on $Rh_2(O_2CR)_4(PY_3)_2^{+\cdot}$.[2a] Summarized data of the intermetallic distance of this class of complexes[14] show general trends that the distance increases when the axial ligand is more σ donative or when the bridging ligand is substituted from acetate to trifluoroacetate, which is consistent with the prediction iv. In parallel to these general trends, the stretching frequency of the intermetallic bond observed in the Raman spectrum of $Rh_2(O_2CMe)_4L_2$ decreases in the order of L = none > MeOH > H_2O > Me_2SO > PPh_3.[15]

Concluding Remarks. The bonding scheme in Figure 7 can qualitatively explain the ligand dependences of intermetallic physicochemical properties of dirhodium tetracarboxylates, showing that this scheme provides, to a first approximation, a good description of the intermetallic bond. In this scheme, intermetallic MO's are expressed as in-phase and anti-phase combinations of "d MO's" in the mononuclear units, which is a consequence of the hypothesis that M–L interactions are greater than M–M interactions.

The π-type interactions between axial ligands and the Rh atom have been generally accepted as minor.[2a,3e,6b,7] The stretching frequency of the carbon monoxide in $Rh_2(O_2CMe)_4(CO)_2$ was reported as 2105 cm^{-1}.[3b] We have observed that of $Rh_2(O_2CCF_3)_4(CO)_2$ at 2150 cm^{-1}. The latter stretching frequency is slightly higher than that of the free carbon monoxide, 2143 cm^{-1}.[16] The σ donation from the carbonyl increases the stretching frequency of the C–O bond[17] whereas the π back-donation results in an enhanced decrease of the frequency. The observed bridging ligand dependence of the carbonyl stretching frequency shows that there is only very small π-type interactions in the C–Rh bond in $Rh_2(O_2CCF_3)_4(CO)_2$ and that in $Rh_2(O_2CMe)_4(CO)_2$ has a minor π-back-bonding character.

Experimental Section

Materials. Ethanol adducts of dirhodium tetrapropionate and dirhodium tetrakis(trifluoroacetate) were prepared by known methods.[18] The propionate was recrystallized from cyclohexane as a pyridine adduct, when necessary. An axial ligand free complex was prepared by heating the ethanol adduct of the trifluoroacetate or pyridine adduct of the propionate for 4–6 h under vacuum at 90 °C for the trifluoroacetate and at 120°C for the propionate. The quinuclidine adduct of a dirhodium tetracarboxylate was prepared by adding a methanol solution of the base to a cold methanol solution of an ethanol adduct in a mole ratio of 2:1. Immediately formed purplish red to reddish brown precipitates were collected and washed with methanol and ether. Preparations of phosphine and phosphite adducts were described earlier,[2a] but the trifluoroacetate complex did not form a stable adduct with tricyclohexylphosphine. Aquo adducts for absorption spectroscopy were generated by dissolving axial ligand free complexes into water solvent.

Electrochemistry. Cyclic voltammetry studies were conducted by using a Hokuto-Denko HB-107A function generator and a HB-104A potentiostat. The electrolyte solution was CH_2CL_2 containing 0.1 mol L^{-1} of n-Bu_4NClO_4 and 1 mmol L^{-1} of a dirhodium complex and was deoxygenated by argon bubbling. Working electrode and counterelectrode were Pt wires. The reference electrode was an SCE.

For measurements of absorption spectra of cation radicals, electrochemical oxidations were performed with the HB-104A potentiostat. The oxidation cell was composed of two compartments connected with a sintered-glass disk. Each compartment has a Au wire as a working electrode or counterelectrode. Electrolyte solution was CH_2Cl_2 containing 0.1 mol L^{-1} of n-Bu_4NClO_4, 0.1–0.4 mmol L^{-1} of a phosphine adduct of dirhodium tetrapropionate, and 1 mmol L^{-1} of the phosphine to suppress the dissociation of the axial ligand. The electrolyte solution in the oxidation compartment was stirred magnetically. When the oxidation current decreased below 5% of the initial current, the oxidation was regarded as completed. After the completion of electrolysis, the electrolyte solution in the oxidation compartment was transferred under air into a quartz optical cell for measurements of absorption spectra of a cation radical. An absorption spectrum due to a cation radical in an electrolyzed solution in an optical cell under air had decayed with a half-life of ca. 0.5 h.

Radiolysis. A deoxygenated Freon mixture ($CFCl_3$:CF_2BrCF_2Br = 1:1 v/v) saturated with a dirhodium complex (several millimoles per liter) was sealed in a quartz cell with a 1.5-mm optical path under vacuum. The absorption spectrum of this solution at 77 K showed no indication of dissociation of the 1:2 adduct into the 1:1 adduct.

(14) Table II of ref 3b and Table VI of ref 3f.
(15) Ketteringham, A. P.; Oldham, C. *J. Chem. Soc., Dalton Trans.* **1973**, 1067.
(16) G. Herzberg, "Molecular Spectra and Molecular Structure"; Van Nostrand-Reinhold: Princeton, NJ, 1950; Vol. I.
(17) The C–O stretching frequency of $OC^{+\cdot}$, which is formed from CO by ionization of an electron from the "carbon lone-pair orbital", is 2184 cm^{-1}.[16]
(18) (a) Rampel, G. A.; Legzdins, P.; Smith, H.; Wilkinson, G.; Ucko, D. A. *Inorg. Synth.* **1972**, *13*, 90. (b) Winkhaus, G.; Ziegler, P. *Z. Anorg. Allg. Chem.* **1967**, *350*, 51.

This Freon mixture solution was exposed to ^{60}Co γ rays at 77 K for several minutes at a dose rate of 5.1×10^{17} eV min^{-1} g^{-1} to generate the cation radical of the solute.

Measurements of Electronic Spectra. Absorption spectra of samples in a quartz cell with a 1- or 10-mm optical path at room temperature were obtained on a Union-Giken SM-401 spectrophotometer. Those at 77 K were measured by using a Cary 17 spectrophotomer equipped with a liquid-nitrogen Dewar vessel with optical windows.

IR Spectrum of $Rh_2(O_2CCF_3)_4(CO)_2$. Axial ligand free $Rh_2(O_2CCF_3)_4$ (187 mg, 0.284 mmol) was kept under carbon monoxide gas of atmospheric pressure at room temperature for 1 h. The weight of the sample increased to 202 mg accompanied by a change in the color from light green to light brown, showing that the 1:2 adduct, $Rh_2(O_2CCF_3)_4(CO)_2$, was formed by absorption of 15 mg (0.55 mmol) of carbon monoxide. KBr pellets of this dicarbonyl adduct were prepared under carbon monoxide gas and transferred for measurements of its IR spectra to a JASCO A-302 infrared spectrophotometer. IR absorptions: 2150 (m), 1644 (s), 1463 (w), 1191 (vs), 862 (m), 784 (m), 739 (s), 544 (m), 527 (sh) cm^{-1}.

Registry No. $Rh_2(O_2CEt)_4(H_2O)_2$, 60801-05-0; $Rh_2(O_2CEt)_4[HC(CH_2CH_2)_3N]_2$, 83416-24-4; $Rh_2(O_2CEt)_4(PPh_3)_2$, 14781-76-1; $Rh_2(O_2CEt)_4[P(c\text{-}C_6H_{11})_3]_2$, 83398-59-8; $Rh_2(O_2CEt)_4[P(OPh)_3]_2$, 83398-60-1; $Rh_2(O_2CEt)_4[P(OMe)_3]_2$, 83398-61-2; $Rh_2(O_2CCF_3)_4(H_2O)_2$, 70084-34-3; $Rh_2(O_2CCF_3)_4[HC(CH_2CH_2)_3N]_2$, 83398-62-3; $Rh_2(O_2CCF_3)_4(PPh_3)_2$, 77966-16-6; $Rh_2(O_2CCF_3)_4[P(c\text{-}C_6H_{11})_3]_2$, 83398-63-4; $Rh_2(O_2CCF_3)_4[P(OPh)_3]_2$, 77966-17-7; $Rh_2(O_2CCF_3)_4[P(OMe)_3]_2$, 83398-64-5.

Contribution from the Department of Chemistry, Brown University, Providence, Rhode Island 02912, and Exxon Research and Engineering Company, Linden, New Jersey 07036

Preparation and Properties of the Systems $Co_{1-x}Ru_xS_2$ and $Rh_{1-x}Ru_xS_2$

J. FOISE, K. KIM, J. COVINO, K. DWIGHT, A. WOLD,* R. CHIANELLI, and J. PASSARETTI

Received January 29, 1982

Members of the systems $Co_{1-x}Ru_xS_2$ ($0 \le x \le 1$) and $Rh_{1-x}Ru_xS_2$ ($0.5 \le x \le 1$) were prepared, and their crystallographic and magnetic properties were studied. From comparison with the system $Co_{1-x}Rh_xS_2$, it appears that the 4d electrons of Rh($4d^7$) are localized in the presence of Co($3d^7$) but delocalized in the presence of Ru($4d^6$). The magnetic susceptibility of the system $Co_{1-x}Ru_xS_2$ is sensitive to the homogeneity of the products and indicates that Ru($4d^6$) behaves as a diamagnetic ion.

Introduction

Numerous studies have reported the effects of cation and anion substitution on the electrical and magnetic properties of CoS_2.[1-10] This compound crystallizes in the cubic pyrite structure (space group *Pa*3) and exhibits metallic ferromagnetism, which has been attributed to a partially filled σ^* band.[11-14] The observed ferromagnetic moment has been reported to be 10% lower than the theoretical value. The reduced moment has been attributed[6] to an overlap of the spin-up and spin-down bands below the Fermi level.

Recently, solid solutions of FeS_2 and NiS_2 with CoS_2 have been made.[6,7] Members of the system $Co_xFe_{1-x}S_2$ exhibit ferromagnetic behavior for $x > 0.05$ with the ferromagnetic moment proportional to the cobalt concentration over the range $0.05 < x < 1.0$. In the $Co_{1-x}Ni_xS_2$ system, antiferromagnetic behavior was observed for $x > 0.1$, although with no well-defined Néel temperature.

Samples of $Cr_xCo_{1-x}S_2$ ($0 \le x < 0.4$) have also been made with use of a high-pressure synthesis.[10] Although the disulfide of chromium is unknown, single-phase pyrite structures were found in the composition range indicated. Magnetic studies of this system showed that the Curie temperature increased rapidly with increasing chromium concentration, to a maximum at about $x = 0.3$, and that the saturation magnetization decreased over a comparable range.

Only one previous study has appeared concerning the substitution of platinum metals for cobalt in CoS_2. Members of the system $Co_{1-x}Rh_xS_2$ ($0 \le x \le 0.6$) were prepared and their magnetic properties studied.[5] It was found that both the Curie temperature and the Weiss constant decreased monotonically with increasing rhodium substitution. At low rhodium concentration, an increase in the ferromagnetic moment (with a maximum at $x = 0.3$) was found and attributed to Co($3d^7$)–Rh($4d^7$) ferromagnetic interactions. As the rhodium concentration was increased further, the moment decreased due to a lack of magnetic homogeneity and the possible formation of rhodium–rhodium clusters.

The purpose of this study is to investigate the magnetic properties of the systems $Co_{1-x}Ru_xS_2$ and $Rh_{1-x}Ru_xS_2$ to further understand the magnetic interactions between cobalt's $3d^7$ electrons and 4d systems.

Experimental Section

Preparation of Materials. Polycrystalline samples of the systems $Co_{1-x}Ru_xS_2$ ($0 \le x \le 1$) and $Rh_{1-x}Ru_xS_2$ ($0.5 \le x \le 1$) were prepared. Attempts to prepare samples by direct combination of the elements were largely unsucessful, but samples were obtained by heating in hydrogen sulfide stoichiometric quantities of pentaamminecobalt(III) chloride and ammonium hexachlororuthenate(IV) for the preparation of members of the system $Co_{1-x}Ru_xS_2$ and ammonium hexachlororhodate(III) and ammonium hexachlororuthenate(IV) for the compositions $Rh_{1-x}Ru_xS_2$.

Direct Combination of the Elements. Starting materials were pretreated as follows: the high-purity metals (Co 99.999%, Leico Inc.; Ru 99.999% and Rh 99.999%, Engelhard Inc.) were reduced in a 15% H_2–85% Ar atmosphere (Co was heated at 650 °C for 4 h, ground, and further reduced at 850 °C for 8 h; Ru and Rh were reduced for 8 h at 800 °C). Freshly sublimed sulfur was used.

Stoichiometric quantities of the elements (with a 10% by weight excess of sulfur) were ground thoroughly and transferred to a silica

* To whom all correspondence should be addressed at Brown University.

(1) Nahigian, H.; Steger, J. J.; Arnott, R. J.; Wold, A. *J. Phys. Chem. Solids* **1974**, *35*, 1349.
(2) Steger, J. J.; Nahigian, H.; Arnott, R. J.; Wold, A. *J. Solid State Chem.* **1974**, *11*, 53.
(3) Johnson, V.; Wold, A. *J. Solid State Chem.* **1970**, *2*, 209.
(4) Mikkelsen, J.; Wold, A. *J. Solid State Chem.* **1971**, *3*, 39.
(5) Covino, J.; Dwight, K.; Wold, A.; Chianelli, R.; Passaretti, J. *Inorg. Chem.* **1982**, *21*, 1744.
(6) Jarrett, H. S.; Cloud, W. H.; Bouchard, R. J.; Butler, S. R.; Frederick, C. G.; Gillson, J. L. *Phys. Rev. Lett* **1968**, *21*, 617.
(7) Bouchard, R. J. *Mater. Res. Bull.* **1968**, *3*, 563.
(8) Adachi, K.; Sato, K.; Takeda, M. *J. Phys. Soc. Jpn.* **1969**, *26*, 631.
(9) Adachi, K.; Sato, K.; Takeda, M. *J. Phys. Soc. Jpn.* **1970**, *29*, 323.
(10) Donohue, P. C.; Bither, T. A.; Cloud, W. H.; Frederick, C. G. *Mater. Res. Bull.* **1971**, *6*, 231.
(11) Bither, T. A.; Bouchard, R. J.; Cloud, W. H.; Donohue, P. C.; Siemons, W. J. *Inorg. Chem.* **1968**, *7*, 2208.
(12) Goodenough, J. B. *J. Appl. Phys.* **1967**, *38*, 1054.
(13) Goodenough, J. B. *J. Solid State Chem.* **1971**, *3*, 26.
(14) Goodenough, J. B. *J. Solid State Chem.* **1972**, *5*, 144.

0020-1669/83/1322-0061$01.50/0